DROSHA targets its own transcript to modulate alternative splicing

DOOYOUNG LEE,[1] JIN-WU NAM,[2] and CHANSEOK SHIN[1,3,4]

[1]Department of Agricultural Biotechnology, Seoul National University, Seoul 08826, Republic of Korea
[2]Department of Life Science, Hanyang University, Seoul 04763, Republic of Korea
[3]Research Institute of Agriculture and Life Sciences, Seoul National University, Seoul 08826, Republic of Korea
[4]Plant Genomics and Breeding Institute, Seoul National University, Seoul 08826, Republic of Korea

ABSTRACT

The nuclear RNase III enzyme DROSHA interacts with its cofactor DGCR8 to form the Microprocessor complex, which initiates microRNA (miRNA) maturation by cleaving hairpin structures embedded in primary transcripts. Apart from its central role in the biogenesis of miRNAs, DROSHA is also known to recognize and cleave miRNA-like hairpins in a subset of transcripts without apparent small RNA production. Here, we report that the human *DROSHA* transcript is one such noncanonical target of DROSHA. Mammalian *DROSHA* genes have evolved a conserved hairpin structure spanning a specific exon–intron junction, which serves as a substrate for the Microprocessor in human cells but not in murine cells. We show that it is this hairpin element that decides whether the overlapping exon is alternatively or constitutively spliced. We further demonstrate that DROSHA promotes skipping of the overlapping exon in human cells independently of its cleavage function. Our findings add to the expanding list of noncanonical DROSHA functions.

Keywords: DROSHA; Microprocessor; alternative splicing

INTRODUCTION

MicroRNAs (miRNAs) are a class of small regulatory RNAs of ~22 nucleotides (nt) involved in diverse biological pathways in bilateral animals. As key regulators of gene expression, they pair with complementary sites within mRNAs and direct post-transcriptional repression of those messages (Bartel 2009). Aberrant miRNA expression is associated with various human diseases, including cancer (Lujambio and Lowe 2012), highlighting the importance of these tiny regulators.

Much is now known about how miRNAs are generated in cells (Ha and Kim 2014). In the canonical biogenesis pathway, miRNA genes are transcribed as primary miRNAs (pri-miRNAs) containing one or more characteristic hairpin structures. These miRNA hairpins are recognized and cleaved by the nuclear Microprocessor complex, a heterotrimeric complex consisting of one molecule of DROSHA, an RNase III, and two molecules of its essential cofactor DiGeorge syndrome critical region 8 (DGCR8), to release ~60- to 80-nt precursor miRNAs (pre-miRNAs) (Lee et al. 2003; Denli et al. 2004; Gregory et al. 2004; Han et al. 2006; Nguyen et al. 2015; Kwon et al. 2016). Pre-miRNAs are then exported to the cytoplasm and further processed by a second RNase III, DICER, producing ~22-base pair (bp) miRNA duplexes (Grishok et al. 2001; Hutvagner et al. 2001). One strand of the duplex is subsequently loaded onto the ARGONAUTE protein to form a functional miRNA-induced silencing complex (miRISC) (Hammond et al. 2001; Mourelatos et al. 2002).

DROSHA plays an irreplaceable role in miRNA biogenesis, as manifested by the complete abolishment of canonical miRNA expression in *DROSHA* knockout (KO) cells (Kim et al. 2016). Human DROSHA contains proline-rich (P-rich) and arginine/serine-rich (RS-rich) domains in the N-terminal region, a central domain (CED) in the middle, and two RNase III domains (RIIIDa and RIIIDb) followed by a double-stranded RNA-binding domain (dsRBD) in the C-terminal region. The N-terminal domains are dispensable for pri-miRNA processing activity in vitro (Han et al. 2004; Nguyen et al. 2015), but appear to provide a regulatory platform for the protein by undergoing multiple post-translational modifications (Tang et al. 2010, 2011, 2013; Yang et al. 2015). For example, phosphorylation of Serine300 and Serine302, located in the RS-rich domain, by glycogen synthase kinase 3β (GSK3β) facilitates nuclear localization of DROSHA (Tang et al. 2010, 2011). On the other hand, several

Corresponding author: cshin@snu.ac.kr
Article is online at http://www.rnajournal.org/cgi/doi/10.1261/rna.059808.116.

serine and threonine residues, including Serine300, are targeted by p38 mitogen-activated protein kinase (MAPK) under stress conditions, leading to nuclear export and subsequent degradation of DROSHA (Yang et al. 2015). The middle and C-terminal domains, in association with two DGCR8 molecules, constitute the catalytic core of the Microprocessor in which RIIIDa and RIIIDb dimerize intramolecularly to cleave the 3′ and 5′ strand of the miRNA hairpin, respectively (Han et al. 2004; Nguyen et al. 2015; Kwon et al. 2016). Recent biochemical and structural studies with purified Microprocessor revealed that DROSHA is the subunit that not only executes the catalysis but also determines the cleavage sites by measuring the distance from the basal junction between single-stranded RNA (ssRNA) and double-stranded RNA (dsRNA) (Nguyen et al. 2015; Kwon et al. 2016).

In addition to its role as the initiator of miRNA maturation, accumulating evidence suggests noncanonical functions of DROSHA (Burger and Gullerova 2015). The homeostatic maintenance of Microprocessor activity relies on the cleavage of pri-miRNA-like hairpin structures embedded in the *DGCR8* mRNA by DROSHA (Han et al. 2009; Kadener et al. 2009; Triboulet et al. 2009). Besides this widespread and deeply conserved targeting, DROSHA directly controls the stability of several mRNAs in particular biological contexts (Kadener et al. 2009; Chong et al. 2010; Karginov et al. 2010; Knuckles et al. 2012; Macias et al. 2012; Johanson et al. 2015). For example, clearance of inhibitory mRNAs in progenitor cells by DROSHA-mediated cleavage has recently emerged as a means of regulating developmental pathways, as illustrated in neurogenesis (Knuckles et al. 2012; Marinaro et al. 2017) and myelopoiesis (Johanson et al. 2015). DROSHA also cleaves and destabilizes viral mRNA (Lin and Sullivan 2011) and retrotransposon transcripts (Heras et al. 2013), serving as a defender against the expression of deleterious elements. Notably, the products of these cleavage events seem unlikely to enter the miRNA pathway, as the corresponding small RNAs could only be detected, if at all, by deep sequencing. Cleavage-independent functions of DROSHA have also been reported, such as regulation of alternative splicing (Havens et al. 2014) and transcriptional activation (Gromak et al. 2013).

Precursor mRNA (pre-mRNA) splicing by the spliceosome and pri-miRNA cleavage by the Microprocessor are two major RNA processing events that occur cotranscriptionally in the nucleus (Pawlicki and Steitz 2010). Because miRNA sequences can be located anywhere in the genome, many primary transcripts serve simultaneously as pre-mRNAs and pri-miRNAs. In this regard, understanding how the two distinct molecular machineries executing each of the processing reactions are coordinated for a single nascent transcript has been an active area of research. Processing of intronic miRNAs, which account for the majority of mammalian miRNAs, generally neither requires nor affects splicing of adjacent exons (Kim and Kim 2007; Kataoka et al. 2009), although a few reports demonstrated the existence of an interplay between the two processes in specific genomic contexts (Janas et al. 2011; Agranat-Tamir et al. 2014). Particularly interesting cases are miRNA hairpins overlapping with exonic sequences. A transcriptome-wide survey of DGCR8 binding sites revealed that DGCR8 makes contact with hundreds of cassette exons, possibly leading to modulation of alternative splicing (Macias et al. 2012). One of the target mRNA identified in this study, *TCF7L1*/*TCF3*, has recently been shown to play a role in stem cell differentiation through DGCR8-dependent alternative splicing control (Cirera-Salinas et al. 2017), underscoring the physiological relevance of the regulation. On the other hand, bioinformatics analysis revealed dozens of miRNAs whose hairpin precursors are located across exon–intron junctions (Mattioli et al. 2013; Melamed et al. 2013). In these situations, the splicing machinery and the Microprocessor compete with each other for a common substrate, although the molecular basis for such competition has remained elusive.

Here, we report that human DROSHA targets and regulates alternative splicing of its own nascent transcript. Mammalian *DROSHA* genes have evolved a conserved hairpin structure spanning the exon 7–intron 7 junction, which serves as a substrate for the Microprocessor complex in human cells but not in murine cells. We show that it is this hairpin element that determines whether *DROSHA* exon 7 is alternatively or constitutively spliced. We further demonstrate that the Microprocessor promotes skipping of exon 7 in human cells primarily through binding to the juxtaposed hairpin rather than cleaving it. Finally, we provide biochemical evidence that the suppressive effect of the Microprocessor on *DROSHA* exon 7 splicing involves sterically hindering the splicing machinery from recognizing its cognate splice site.

RESULTS

The *DROSHA* hairpin

While examining deep sequencing data of small RNAs expressed in HeLa cells (Shin et al. 2010), we observed two sets of reads mapped across the exon 7–intron 7 junction of the *DROSHA* pre-mRNA (Fig. 1A). These sets of reads were reminiscent of miRNA duplexes in that they were complementary to each other with 3′ overhangs and were predicted to constitute the apical stem of a hairpin structure (Fig. 1B). Searching for potential repetitive elements near the corresponding genomic region revealed the presence of a palindromic sequence likely derived from medium reiteration frequency 5A (MER5A) transposons (Fig. 1C). We annotated this 190-nt element as the human *DROSHA* hairpin. To investigate whether the *DROSHA* hairpin is evolutionarily conserved, we inspected the orthologous genomic regions of other vertebrate *DROSHA* genes. We found similar palindromic sequences in the genomes of most placental mammals, but not in those of chicken, frog, and zebrafish (Fig. 1B,C; Supplemental Fig. 1).

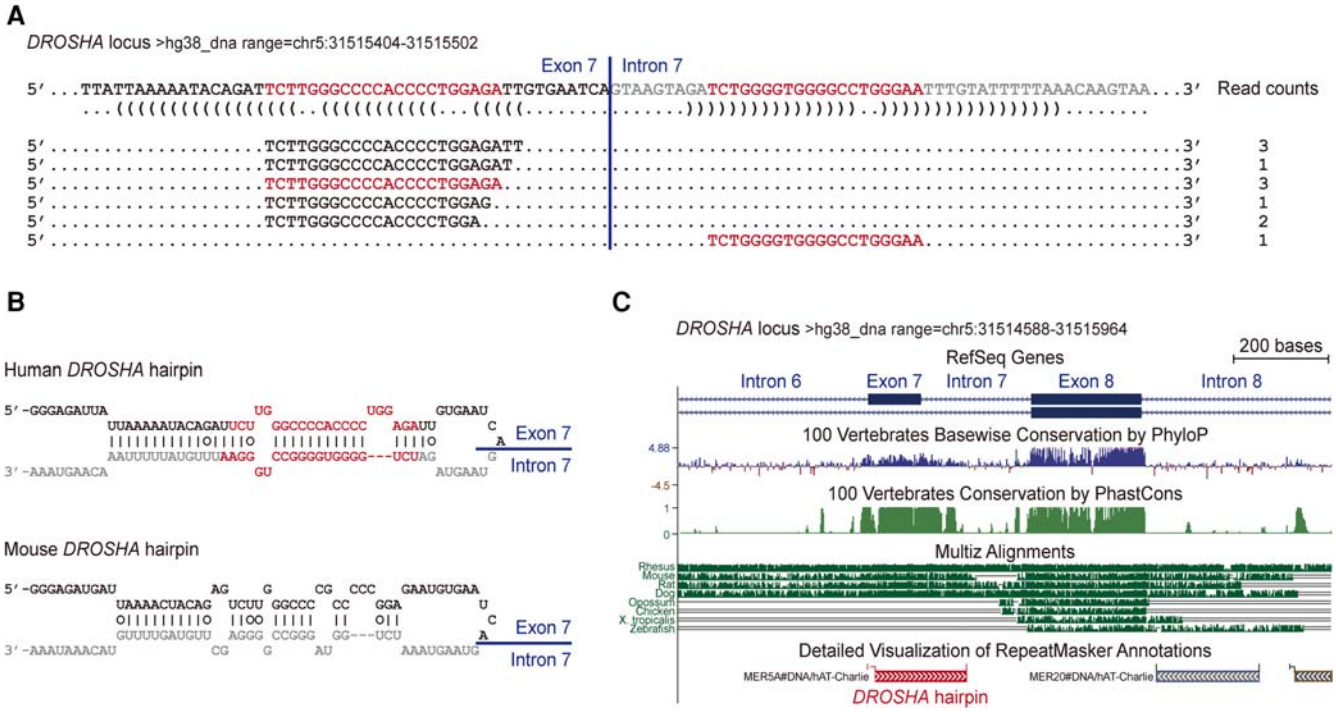

FIGURE 1. Structure and conservation of the *DROSHA* hairpin. (*A*) HeLa small RNA reads mapped across the exon 7–intron 7 junction of the *DROSHA* pre-mRNA (Shin et al. 2010). The dominantly abundant small RNA species of each set is marked in red. Exonic and intronic sequences are presented in black and gray, respectively. (*B*) Predicted secondary structures of the human and mouse *DROSHA* hairpins, colored as in *A*. Prediction was performed using the mfold RNA-folding algorithm (Zuker 2003). (*C*) Evolutionary conservation of the *DROSHA* hairpin as shown in the UCSC Genome Browser (https://genome.ucsc.edu/). The *DROSHA* hairpin is indicated by a red bar.

The human *DROSHA* hairpin is cleaved by the Microprocessor in vitro and in vivo

Semblance of the *DROSHA* hairpin to pri-miRNAs raised the possibility that DROSHA may target its own transcript. First, we addressed whether the *DROSHA* hairpin could be cleaved by the Microprocessor complex in vitro. When human *DROSHA* hairpin RNA was incubated with Microprocessor lysate, prepared from HEK293T cells overexpressing both DROSHA and DGCR8, an ~60-nt fragment was generated, demonstrating that this hairpin served as a genuine substrate for the Microprocessor in vitro (Fig. 2A). To rule out the possibility that the observed cleavage was due to an endoribonuclease other than DROSHA, we performed in vitro processing with a lysate containing an overexpressed DROSHA mutant, E110bQ. This DROSHA mutant, which carries a point mutation in RIIIDb and is, therefore, only capable of cleaving the 3′ strand of a hairpin, released a larger (~140 nt) fragment, as expected (Fig. 2A). We cloned and sequenced the ~60-nt fragment generated from the human *DROSHA* hairpin to clarify its identity. The majority of clones (26 of 31) revealed cleavage sites consistent with Microprocessor-mediated processing, which leaves two staggered cuts approximately one helical turn (~11 bp) away from the basal ssRNA-dsRNA junction (Fig. 2B; Zeng et al. 2005; Han et al. 2006; Auyeung et al. 2013).

In stark contrast, the mouse *DROSHA* hairpin failed to be processed by any of the lysates despite its overall sequence and structural similarities to the human hairpin (Fig. 2A). We excluded the possibility of murine-specific factor(s) required for efficient processing of the mouse hairpin, because in vitro processing with a lysate or the endogenous Microprocessor immunopurified from mouse embryonic fibroblasts gave similar results (data not shown). This failure may be because of suboptimal stem length of or multiple mismatches in the mouse hairpin (Fig. 1B; Fang and Bartel 2015). To examine whether the processing defect is coupled to the lack of Microprocessor binding, we carried out in vitro RNA pulldown assay. Hairpin RNAs immobilized on agarose beads were incubated with HEK293T lysates containing the components of a catalytically deficient Microprocessor (*trans*-dominant negative [TN] DROSHA and/or DGCR8), and proteins specifically bound to the RNA were analyzed by Western blotting. Consistent with the results from in vitro processing, only the human *DROSHA* hairpin efficiently precipitated the Microprocessor or its dsRNA-binding subunit DGCR8 (Fig. 2C). Of note, TN DROSHA interacted with the human *DROSHA* hairpin only in the presence of DGCR8, emphasizing the role of DGCR8 as an obligate partner for DROSHA (Gregory et al. 2004; Han et al. 2004, 2006; Nguyen et al. 2015).

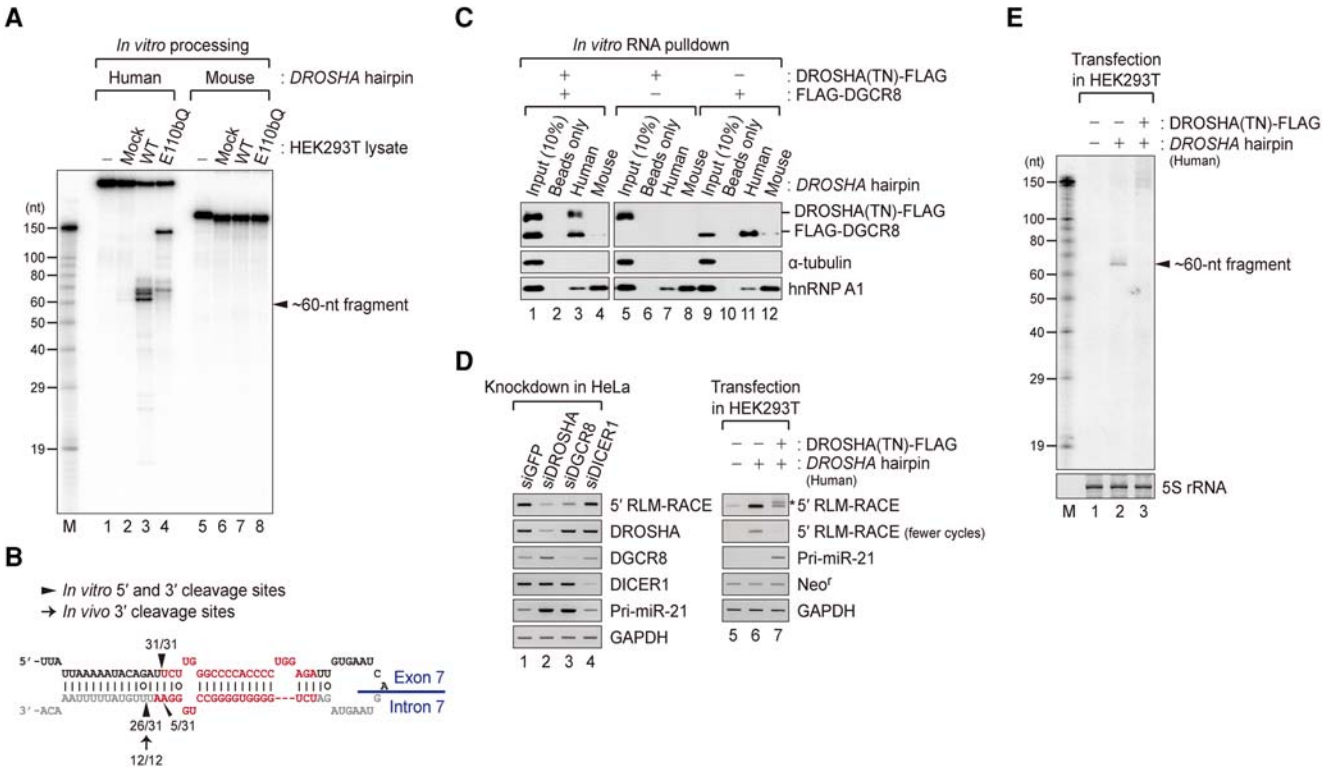

FIGURE 2. The human *DROSHA* hairpin is cleaved by the Microprocessor complex in vitro and in vivo. (*A*) In vitro processing of the *DROSHA* hairpin with Microprocessor lysates. Radiolabeled hairpin RNAs were incubated with lysates from HEK293T cells overexpressing either a wild-type (WT) or mutant (E110bQ) version of the Microprocessor. The pre-miRNA-like processing product of ~60-nt is indicated by an arrowhead. (*B*) Determination of cleavage sites in the human *DROSHA* hairpin. The ~60-nt fragment from in vitro processing was gel-purified, cloned, and sequenced to determine the 5′ and 3′ cleavage sites (arrowhead). The in vivo 3′ cleavage site, as identified by cloning of the 5′ RLM-RACE product from HeLa cells, is also indicated (arrow). (C) In vitro RNA pulldown with the *DROSHA* hairpin. Cold hairpin RNAs covalently attached to agarose beads were incubated with lysates from HEK293T cells overexpressing the components of the Microprocessor, and bound proteins were analyzed by Western blotting. Tubulin serves as a negative control for pulldown. hnRNP A1 was used as a positive control, which turned out by mass spectrometric analyses to interact with both hairpin RNAs (data not shown). (*D*) 5′ RLM-RACE experiments to capture the 3′ processing product. Total RNAs from HeLa cells depleted of DROSHA, DGCR8, or DICER1 were subjected to 5′ RLM-RACE (*left* panel). PCR amplification was terminated in the linear phase (45 cycles) and nested PCR was omitted to prevent signal saturation. The accumulation of *DGCR8* mRNA in DROSHA-depleted cells and of pri-miR-21 in DROSHA- or DGCR8-depleted cells confirms the functional knockdown of each protein. 5′ RLM-RACE results for HEK293T cells overexpressing either the human *DROSHA* hairpin alone or both the hairpin and TN DROSHA are also shown (*right* panel). Derepression of pri-miR-21 serves as a positive control for TN DROSHA expression. Expression of the neomycin resistance gene (Neo^r), which is encoded in the hairpin expression construct, reflects the transfection efficiency. The *upper* band marked with an asterisk is a heteroduplex species associated with overamplification. (*E*) Small RNA Northern blot analysis to detect processing products from the human *DROSHA* hairpin. The ~60-nt processing product is indicated by an arrowhead. Ethidium bromide staining of 5S rRNA serves as a loading control.

Next, we asked whether Microprocessor-mediated cleavage of the human *DROSHA* hairpin actually occurs in cells. We utilized RNA ligase-mediated rapid amplification of cDNA 5′ ends (5′ RLM-RACE) to capture the 3′ processing product of the hairpin (Karginov et al. 2010; Shin et al. 2010). A reverse primer was designed to hybridize to human intron 7, and 5′ RLM-RACE was performed on total RNA isolated from HeLa cells. RACE amplified a product of the expected size (Fig. 2D), which mapped the same 3′ cleavage site as determined by in vitro experiments (Fig. 2B). Notably, the intensity of the RACE product was markedly reduced when either DROSHA or DGCR8 was depleted by RNAi, suggesting a specific role of the Microprocessor in this cleavage event (Fig. 2D). Knockdown of DICER, another RNase III implicated in miRNA biogenesis, had no effect on the RACE signal. To further confirm that the RACE product indeed originated from the human *DROSHA* hairpin in a DROSHA-dependent manner, we transfected HEK293T cells with a plasmid in which the hairpin and its surrounding genomic sequences were placed under the control of the CMV promoter. Ectopic expression of the human *DROSHA* hairpin RNA gave rise to an intensified RACE product of exactly the same size, which was substantially diminished upon coexpression of TN DROSHA (Fig. 2D). We also performed Northern blot analysis to detect the ~60-nt processing product or the ~22-nt small RNA derived from it. We failed to observe any species on the blot when we used total RNA from mock-transfected HEK293T cells, indicating that the steady-state level of the processing product is generally low in normal conditions. However, overexpression of the

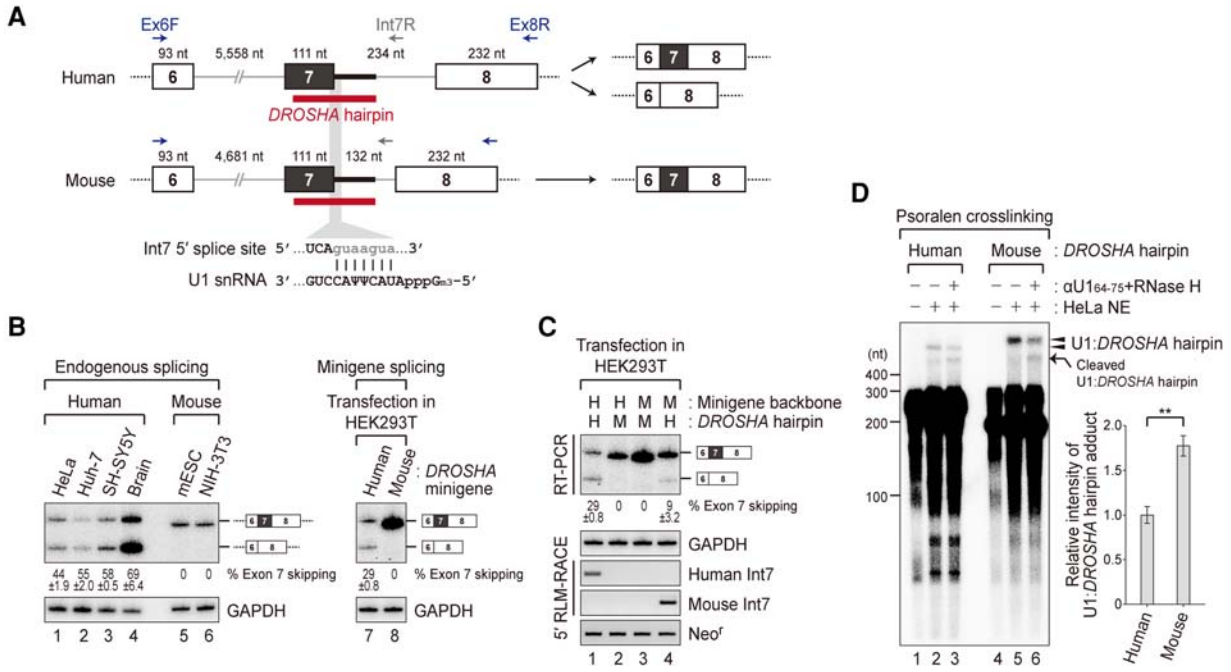

FIGURE 3. The human *DROSHA* hairpin is responsible for alternative splicing of *DROSHA* exon 7. (*A*) Schematic representation of the *DROSHA* gene region from exons 6–8. Boxes, *horizontal* lines, and the red bar across the exon 7–intron 7 junction depict exons, introns, and the *DROSHA* hairpin, respectively. PCR primers to detect exon 7 splicing or the 3′ processing product are represented by blue and gray arrows, respectively. It is noted that a vector-specific forward primer was used instead of Ex6F for the analysis of minigene splicing. The 5′ splice site of intron 7 and its base-pairing to U1 snRNA are also shown. (*B*) Splicing of *DROSHA* exon 7 in human and murine cells and its recapitulation in minigene systems. Percentages of the exon 7-skipped isoform and standard error of the mean (SEM) from three independent experiments are presented *below* the gel. (*C*) Hairpin swapping assay. The *DROSHA* hairpins were interchanged between the human and mouse minigenes and exon 7 splicing from these hybrid constructs was analyzed. H and M stand for human and mouse, respectively. 5′ RLM-RACE was also performed to indicate hairpin cleavage in cells. Percentages of the exon 7-skipped isoform and SEM from three biologically independent experiments are presented *below* the gel. GAPDH and Neo^r serve as loading controls. (*D*) Psoralen crosslinking assay. Radiolabeled hairpin RNAs were incubated with HeLa nuclear extract (NE) under splicing conditions and irradiated with 365-nm UV light in the presence of psoralen. The U1 snRNA:*DROSHA* hairpin adducts are indicated by arrowheads. The shortened adducts resulting from RNase H digestion with an oligonucleotide complementary to U1 snRNA are marked by an arrow. Relative intensities of the adducts from five independent experiments are plotted on the graph. (**) Statistical significance of $P \leq 0.005$ as determined by Student's *t*-test. Error bars represent SEM.

hairpin led to an accumulation of the ~60-nt fragment, which was no longer visible after TN DROSHA coexpression (Fig. 2E). Taken together, these results indicate that the human *DROSHA* hairpin is cleaved by the Microprocessor in vivo as well as in vitro.

It is of note that, even when we overexpressed the human *DROSHA* hairpin, we could barely detect the ~22-nt small RNA (Fig. 2E). This is consistent with the low number of sequencing reads mapped across the hairpin (Fig. 1A). Several reports have demonstrated that Microprocessor-mediated cleavage can be decoupled from miRNA biogenesis (Han et al. 2009; Triboulet et al. 2009; Knuckles et al. 2012; Johanson et al. 2015). One prominent example is a hairpin structure embedded in the 5′-untranslated region (5′-UTR) of the *DGCR8* mRNA, which is cleaved by the Microprocessor to generate an ~60-nt RNA fragment that is largely confined to the nucleus (Han et al. 2009). However, the ~60-nt processing product from the ectopically expressed human *DROSHA* hairpin was exported to the cytoplasm as efficiently as a canonical pre-miRNA, pre-miR-143, suggesting that further processing defects exist downstream from nuclear export (Supplemental Fig. 2A). For example, a trinucleotide bulge positioned in the apical stem of the hairpin may impair DICER processing, because filling this bulge dramatically enhanced small RNA production (Supplemental Fig. 2B).

The human *DROSHA* hairpin is responsible for the skipping of *DROSHA* exon 7

Interestingly, exon 7 of the human *DROSHA* mRNA, which comprises the 5′ half of the human *DROSHA* hairpin, is annotated as an alternative exon (Fig. 3A). At the time of writing, RefSeq catalogs 11 splice isoforms for the human *DROSHA* gene, four of which lack exon 7 (NM_001100412.1, XM_017009401.1, XM_005248294.3, and XM_017009400.1) because of alternative splicing. In contrast, skipping of *DROSHA* exon 7 is not conserved in mouse; in RefSeq, all four mouse *DROSHA* transcripts contain exon 7. To validate this species-specific alternative

splicing, we performed radioactive RT-PCR analysis using a panel of total RNAs of human (HeLa, Huh-7, SH-SY5Y, and whole brain) or mouse (mESC and NIH-3T3) origin. Amplification of the region between exons 6 and 8 from human cDNAs resulted in two distinct bands, which proved by cloning and sequencing to be splice isoforms differing in the presence or absence of exon 7 (Fig. 3B). It is noted that the relative abundance of the two isoforms varies substantially among different tissues, with the exon 7-skipped isoform being predominantly expressed in the brain (Supplemental Fig. 3). On the other hand, mouse cDNAs produced only one band corresponding to the full-length transcript, confirming constitutive splicing of *DROSHA* exon 7 in murine cells (Fig. 3B).

Given the importance of RNA secondary structure in the regulation of splicing (Jin et al. 2011; McManus and Graveley 2011), we speculated that the *DROSHA* hairpin may play a key role in determining whether, and if so, to what extent, exon 7 is skipped. To explore this possibility, we constructed splicing reporter minigenes by subcloning the genomic fragment spanning *DROSHA* exons 6–8 downstream from the CMV promoter. When transfected into HEK293T cells, these minigenes faithfully recapitulated the splicing patterns of their endogenous counterparts; the human *DROSHA* minigene produced both the full-length and exon 7-skipped isoforms, whereas the mouse minigene exclusively generated the full-length transcript (Fig. 3B). Next, we reciprocally swapped the *DROSHA* hairpin elements between the human and mouse minigenes and introduced these hybrid constructs into HEK293T cells. 5′ RLM-RACE experiments with reverse primers complementary to the diverged region of intron 7 demonstrated that only the human *DROSHA* hairpin was cleaved regardless of the surrounding genomic sequences (Fig. 3C). Notably, the human *DROSHA* minigene containing the mouse *DROSHA* hairpin no longer displayed exon 7 skipping. In contrast, the mouse minigene bearing the human *DROSHA* hairpin started to alternatively splice exon 7 (Fig. 3C). Similar results were obtained when we used HeLa cells or NIH-3T3 cells as transfection hosts, indicating that the fate of exon 7 as an alternative or a constitutive exon is dictated by primary sequence determinants in the minigenes rather than by cell type-specific or species-specific splicing factors (Supplemental Fig. 4). Of note, we reproducibly observed that skipping of exon 7 from the hybrid minigene was relatively inefficient compared to that from the wild-type human minigene (Fig. 3C; Supplemental Fig. 4). This indicated that additional *cis*-acting elements outside of the *DROSHA* hairpin may be in operation to modulate exon 7 splicing, for example, splicing enhancers in the murine genomic context. Nevertheless, these data strongly demonstrated that it is the *DROSHA* hairpin that makes the decision of whether to splice exon 7 alternatively or constitutively.

The human and mouse *DROSHA* hairpins exhibit ~84% nucleotide sequence identity, with the same 9-mer core sequence representing the 5′ splice site of intron 7 (5′-UCAguaagu-3′, where the 3′ sequence of exon 7 is presented in uppercase) (Fig. 3A). We speculated that the same 5′ splice site may have differential affinity to U1 small nuclear ribonucleoprotein (U1 snRNP) in the context of the two different hairpins, possibly contributing to the different fates of exon 7. To test this, we measured U1 snRNP binding to the *DROSHA* hairpins in HeLa nuclear extract by psoralen crosslinking assay, which allows the detection of RNA–RNA interactions (Nilsen 2014). When *DROSHA* hairpin RNAs were incubated with HeLa nuclear extract and irradiated with long-wavelength UV light in the presence of psoralen, additional species migrating more slowly than the substrate were observed for both the human and mouse hairpins (Fig. 3D). RNase H digestion of the purified crosslinking reactions with a DNA oligonucleotide targeting the second loop of U1 snRNA (nt 64–75) increased the mobility of those species (Fig. 3D), indicating that they represent the *DROSHA* hairpins crosslinked to U1 snRNA. Notably, the human *DROSHA* hairpin reproducibly generated less intense signals for U1 snRNA-crosslinked species than the mouse hairpin (Fig. 3D), which supports our conclusion that the human, but not mouse, hairpin directs exon 7 skipping despite the identical 5′ splice site sequence shared by the two hairpins (Fig. 3C). It is possible that evolutionary nucleotide substitutions in the *DROSHA* hairpin may have disrupted or created *cis*-acting regulatory elements, thereby changing the repertoire of bound splicing factors and enabling differential recognition of the same 5′ splice site by U1 snRNP. Another nonmutually exclusive possibility is that alterations in the secondary structure of the *DROSHA* hairpin RNA may be responsible for the differential exon 7 selection. Supporting this idea, RNA secondary structure prediction revealed that the human *DROSHA* hairpin forms much more stable structures compared to those of the mouse hairpin (ΔG = approximately −93 to −90 kcal/mol for the human *DROSHA* hairpin; ΔG = approximately −67 to −63 kcal/mol for the mouse *DROSHA* hairpin) (Supplemental Fig. 1). Extensive intramolecular pairing in the human *DROSHA* hairpin may sequester splicing regulatory signals to some extent to drive exon 7 skipping.

The Microprocessor modulates alternative splicing of human *DROSHA* exon 7 independently of *DROSHA* hairpin cleavage

The observations that the human *DROSHA* hairpin is cleaved by the Microprocessor and that this element is necessary and sufficient to direct *DROSHA* exon 7 skipping prompted us to propose that the Microprocessor may modulate alternative splicing of human *DROSHA* exon 7. Two recent studies demonstrated the existence of miRNAs whose hairpin precursors overlap with exon–intron junctions (Mattioli et al. 2013; Melamed et al. 2013). In these situations, the splicing machinery and the Microprocessor competed with each other

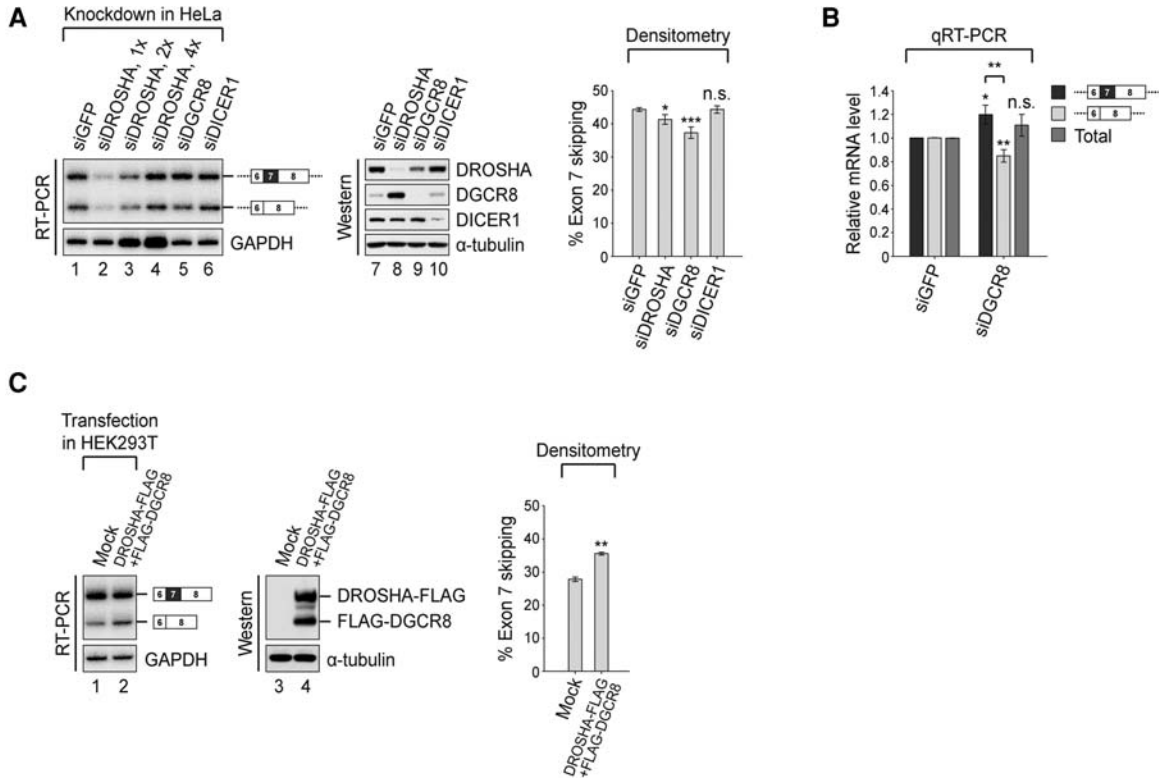

FIGURE 4. The Microprocessor regulates alternative splicing of human *DROSHA* exon 7. (*A*) Endogenous splicing of *DROSHA* exon 7 in HeLa cells depleted of DROSHA, DGCR8, or DICER. For DROSHA knockdown, increasing amounts of cDNA were used in amplification to obtain band intensities that were similar to those of the other samples. Percentages of the exon 7-skipped isoform from five biologically independent experiments are plotted on the graph. (*B*) qRT-PCR measurement of splice isoforms in DGCR8-depleted HeLa cells. Primers spanning specific exon–exon junctions were used to quantify each splice isoform individually. The total *DROSHA* mRNA level was measured by amplifying the region between exons 29 and 30. Relative transcript levels from five biologically independent experiments are plotted on the graph. (*C*) Splicing of the human *DROSHA* minigene in HEK293T cells following overexpression of the Microprocessor. Percentages of the exon 7-skipped isoform from three biologically independent experiments are plotted on the graph. (*) $P \leq 0.05$, (**) $P \leq 0.005$, and (***) $P \leq 0.0005$ indicate statistical significance as determined by Student's *t*-test. n.s., not significant. Error bars represent SEM.

for a single nascent transcript, such that knockdown of DROSHA or DGCR8 led to increased exon inclusion. To test whether similar regulation is operational on the human *DROSHA* hairpin, we depleted the components of the Microprocessor in HeLa cells by RNAi and investigated endogenous splicing patterns of *DROSHA* exon 7. Reduction of Microprocessor activity indeed resulted in increased inclusion of *DROSHA* exon 7, suggesting that the Microprocessor interfered with splicing of this alternative exon (Fig. 4A). The change in alternative splicing was not due to a loss of small RNAs, as depletion of DICER did not alter the ratio of the two splice isoforms. Interestingly, we reproducibly observed a stronger effect on exon 7 splicing by knocking down DGCR8, compared with DROSHA, which may be explained by the well-established cross-regulation between DROSHA and DGCR8 (Han et al. 2009; Kadener et al. 2009; Triboulet et al. 2009). As DGCR8 stabilizes the DROSHA protein through protein–protein interactions (Han et al. 2009; Nguyen et al. 2015; Kwon et al. 2016), knockdown of DGCR8 decreases the protein levels of both DROSHA and DGCR8 (Fig. 4A). On the other hand, depletion of DROSHA causes significant up-regulation of the level of DGCR8 protein (Fig. 4A), which alone is capable of binding to the human *DROSHA* hairpin (Fig. 2C). The increased free DGCR8 molecules in DROSHA-depleted cells may adversely affect exon 7 inclusion and partially compensate for the reduction of Microprocessor activity.

It has been suggested that the 5′ and 3′ flanking fragments generated by Microprocessor-mediated processing are rapidly degraded by exonucleases such as XRN2 and nuclear exosome (Morlando et al. 2008; Ballarino et al. 2009). In this regard, it is possible that Microprocessor activity promotes degradation of exon 7-containing nascent transcripts and thereby simply overrepresents the level of the exon 7-skipped isoform in conventional RT-PCR, rather than actually regulating exon 7 splicing. To test this possibility, we measured the relative abundance of each splice isoform in mock- or DGCR8-depleted HeLa cells by quantitative RT-PCR (qRT-PCR) experiments. Notably, knockdown of DGCR8 not only up-regulated the level of the exon 7-containing isoform, but it also down-regulated the level of the exon 7-skipped isoform without altering the level of total *DROSHA* mRNAs

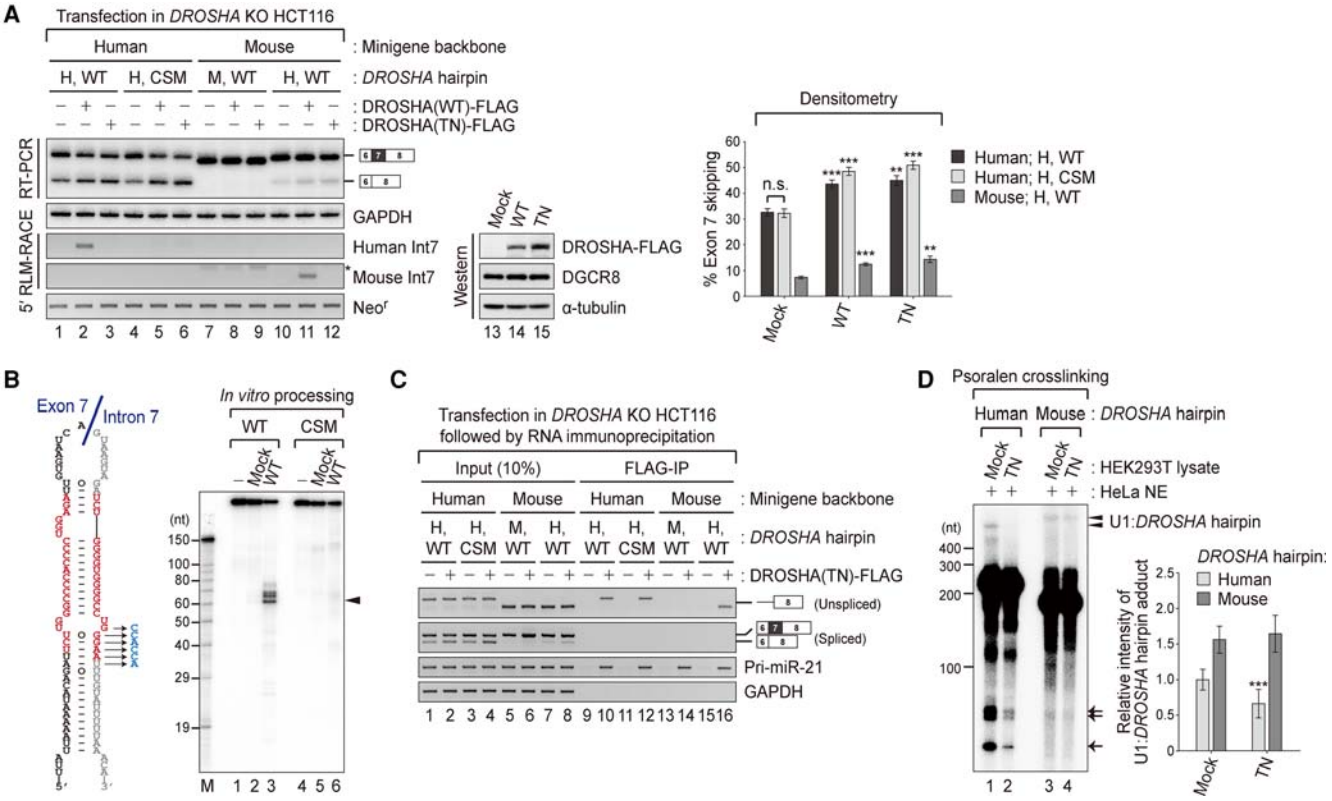

FIGURE 5. The Microprocessor-mediated suppression of *DROSHA* exon 7 splicing occurs independently of *DROSHA* hairpin cleavage. (*A*) Minigene splicing in *DROSHA* KO HCT116 cells replenished with wild-type (WT) or catalytically inactive (TN) DROSHA. H and M stand for human and mouse, respectively. 5′ RLM-RACE was performed to indicate hairpin cleavage in cells. The *upper* band marked with an asterisk indicates a non-specific amplification product independent of hairpin cleavage. GAPDH and Neo^r serve as loading controls. Percentages of the exon 7-skipped isoform from three biologically independent experiments are plotted on the graph. (**) $P \leq 0.005$ and (***) $P \leq 0.0005$ indicate statistical significance as determined by Student's *t*-test. n.s., not significant. Error bars represent SEM. (*B*) Cleavage site mutant (CSM) of the human *DROSHA* hairpin. The 3′ cleavage site was mutated at the indicated positions to disrupt base-pairing, which effectively prevented Microprocessor-mediated cleavage, as confirmed by the in vitro DROSHA processing assay. (*C*) RNA immunoprecipitation assay. Transfected *DROSHA* KO HCT116 cells were crosslinked with formaldehyde, lysed, and subjected to immunoprecipitation using an anti-Flag antibody. Coprecipitated RNA was analyzed by RT-PCR. H and M stand for human and mouse, respectively. An intron 7-specific forward primer and a vector-specific reverse primer were used to detect nascent transcripts. Pri-miR-21 and GAPDH serve as positive and negative controls for DROSHA-Flag immunoprecipitates, respectively. (*D*) Psoralen crosslinking assay in the presence of Microprocessor lysate. Binding reactions for crosslinking were supplemented with mock or Microprocessor lysate containing TN DROSHA. The U1 snRNA:*DROSHA* hairpin adducts are indicated by arrowheads. The fragments generated by Microprocessor-mediated cleavage of the human *DROSHA* hairpin are indicated by arrows. Relative intensities of the adducts from five independent experiments are plotted on the graph. (***) Statistical significance of $P \leq 0.0005$ as determined by Student's *t*-test. Error bars represent SEM.

(Fig. 4B), which is expected if the observed effect of the Microprocessor on *DROSHA* exon 7 splicing represents true regulation rather than simple degradation.

To confirm the result from the knockdown experiments, we transiently transfected HEK293T cells with the human *DROSHA* minigene and examined splicing patterns in the presence of additional DROSHA and DGCR8 proteins. Overexpression of the Microprocessor caused a shift in minigene splicing toward exon 7 skipping, confirming the inhibitory role of this complex in the splicing of *DROSHA* exon 7 (Fig. 4C).

In principle, the Microprocessor-mediated cleavage of miRNA hairpins that are juxtaposed with splice sites would make the overlapping exons permanently unavailable for splicing. To investigate whether cleavage of the *DROSHA* hairpin is required for exon 7 skipping, we introduced the human *DROSHA* minigene into *DROSHA* KO HCT116 cells in which Microprocessor activity is completely extinguished (Kim et al. 2016). Exon 7 was still spliced alternatively in *DROSHA* KO cells, indicating that hairpin cleavage per se is not a prerequisite for exon 7 skipping (Fig. 5A). Furthermore, replenishment of KO cells with TN DROSHA, which is catalytically inert, as well as wild-type DROSHA, tilted minigene splicing in favor of exon 7 skipping to similar extents, demonstrating that the catalytic activity of DROSHA is dispensable for promoting exon 7 skipping (Fig. 5A). We also generated a minigene in which the cleavage site of the human *DROSHA* hairpin was mutated to prevent Microprocessor-mediated processing (Fig. 5B). Notably, the minigene bearing the cleavage site mutant (CSM) *DROSHA*

hairpin produced the two splice isoforms and responded to coexpression of wild-type or TN DROSHA in *DROSHA* KO cells very similarly to the wild-type minigene (Fig. 5A). The nascent transcripts from both minigenes were precipitated by TN DROSHA as efficiently and specifically as an endogenous target, pri-miR-21, suggesting that the observed effect of DROSHA on splicing regulation likely emanated from its physical interactions with RNA (Fig. 5C).

To be certain that the human *DROSHA* hairpin is responsible for the splicing inhibition and binding of the minigene transcript by DROSHA, we examined the behaviors of the mouse *DROSHA* minigene and its hybrid mutant containing the human *DROSHA* hairpin in *DROSHA* KO cells. While the mouse minigene was neither differentially spliced upon DROSHA overexpression nor bound by DROSHA as anticipated, transplantation of the human *DROSHA* hairpin allowed the hybrid minigene to respond to and interact with DROSHA in the same way that the human minigenes did (Fig. 5A,C). Taken together, these data indicate that the Microprocessor impedes splicing of *DROSHA* exon 7 in human cells primarily through binding to the *DROSHA* hairpin rather than cleaving it.

Given that the catalytic activity of DROSHA is dispensable for regulating exon 7 splicing, we speculated that the Microprocessor may promote exon 7 skipping by occupying the human *DROSHA* hairpin and sterically hindering U1 snRNP from recognizing the 5′ splice sites. To investigate this possibility, we supplemented binding reactions for psoralen crosslinking with either mock or Microprocessor lysate containing TN DROSHA. Addition of Microprocessor lysate significantly impaired cleavage of the human *DROSHA* hairpin by endogenous DROSHA (Fig. 5D), indicating the existence of robust interactions between exogenous TN DROSHA and the human hairpin. Notably, crosslinking to U1 snRNA was substantially diminished under these conditions only for the human *DROSHA* hairpin (Fig. 5D), which was expected from our hypothesis. This observation demonstrates that the restricted access of U1 snRNP to the 5′ splice site mediated by the Microprocessor contributes to the suppressive effect of this complex on human *DROSHA* exon 7 splicing.

DISCUSSION

In this study, we examined the role of a specific structural element, the *DROSHA* hairpin, in the regulation of alternative splicing. The *DROSHA* hairpin is comprised of a genomic region that spans the junction between exon 7 and intron 7 of the *DROSHA* pre-mRNA and is evolutionarily conserved among placental mammals (Fig. 1). In human cells, this hairpin is recognized and cleaved by the Microprocessor complex, the catalytic subunit of which is DROSHA (Fig. 2). Such targeting is not observed in murine cells despite overall sequence and structural homologies between the human and mouse hairpins (Figs. 1, 2). We demonstrated that the human *DROSHA* hairpin is necessary and sufficient to direct skipping of *DROSHA* exon 7, which occurs in human cells but not in murine cells (Fig. 3). Based on these findings, we showed that the Microprocessor promotes exon 7 skipping in human cells and that this effect mainly stems from Microprocessor binding to the *DROSHA* hairpin rather than hairpin cleavage (Figs. 4, 5).

The *DROSHA* hairpin is classified by RepeatMasker as a derivative of MER5A transposable elements, which emerged in placental mammals (Fig. 1C). The palindromic nature of many transposons makes them plausible candidates for the evolutionary origin of miRNA genes (Piriyapongsa et al. 2007; Roberts et al. 2014; Qin et al. 2015). For example, the placental-specific miR-1302 family was recently proposed to have originated from MER53 transposons (Yuan et al. 2010). It is noteworthy that one repeat element introduced in the last common ancestor has diverged in some species to serve as a hairpin precursor for miR-1302, while in other species it has remained biologically inert (Yuan et al. 2010). This is strongly reminiscent of the *DROSHA* hairpin, which is cleaved by the Microprocessor in human cells but not in murine cells (Fig. 2). Analogous to the miR-1302 hairpins, the *DROSHA* hairpin may have acquired regulatory potential in a species-specific manner.

Recently, two independent groups systematically identified dozens of annotated miRNAs whose hairpin precursors are located across exon–intron junctions (Mattioli et al. 2013; Melamed et al. 2013). By using minigene assays and extensive mutagenesis studies, they experimentally validated functional antagonism between the splicing machinery and the Microprocessor, which we also observed in the case of the human *DROSHA* hairpin (Figs. 4, 5). In line with these findings, we provided biochemical evidence that the suppressive effect of the Microprocessor on *DROSHA* exon 7 splicing does not depend on the catalytic activity of DROSHA and involves sterically hindering the splicing machinery from recognizing its cognate splice site (Fig. 5). Further studies are needed to reveal whether similar mechanisms operate in other cases of splice-site-overlapping miRNAs.

Interestingly, it appears that the Microprocessor does not always compete with the splicing machinery when they share a common substrate. For example, the alternatively spliced exon 5 of the *eIF4H* pre-mRNA folds into a pri-miRNA-like hairpin structure, which is cleaved by DROSHA in vitro and in cells (Havens et al. 2014). However, the primary role of DROSHA here is to promote inclusion of exon 5 through an as-yet-uncharacterized, cleavage-independent mechanism (Havens et al. 2014). Processing of the miR-211 hairpin present in intron 6 of the *TRPM1* pre-mRNA stimulates splicing of adjacent exons (Janas et al. 2011). DGCR8 binds to a hairpin structure embedded in intron 4 of the *TCF7L1*/*TCF3* pre-mRNA and ensures the correct splicing, which is necessary for the differentiation of mouse embryonic stem cells (Cirera-Salinas et al. 2017). These findings are hard to digest with the currently known functions of the

Microprocessor, but may be supported by physical association between the spliceosome and the Microprocessor components (Gregory et al. 2004; Kataoka et al. 2009; Agranat-Tamir et al. 2014). It will be interesting to investigate the detailed mechanisms by which the Microprocessor facilitates splicing and to draw underlying commonalities from these seemingly unrelated regulatory events.

In vertebrate DROSHA, exons 5 to 8 encode the N-terminal RS-rich domain, the function of which is largely unexplored. What are the biological consequences of *DROSHA* exon 7 skipping? It is noted that the majority of exon 7 sequences overlap with the 5′ half of the *DROSHA* hairpin (Fig. 1C), suggesting a coevolution of exon 7 with the hairpin. Consistent with this idea, exon 7 is found only in placental mammals while the neighboring exons are traceable in non-mammalian vertebrates, including chicken, frog, and zebrafish, as well as in mammals (Supplemental Fig. 5). Possibly reflecting its relatively recent emergence, we noticed that the protein region encoded by exon 7 exhibits slightly different physicochemical properties. For example, exon 7 encodes several hydrophobic amino acid residues, which creates a local hydrophobic patch within the long hydrophilic stretch of the RS-rich domain (Supplemental Fig. 5). The RS-rich domains found in many splicing factors are primarily involved in protein–protein interactions (Long and Caceres 2009; Shepard and Hertel 2009); therefore, interruption of RS-rich domain hydrophilicity by the presence of exon 7 may change the repertoire of interaction partners for DROSHA, which has indeed been shown to associate with a variety of auxiliary cofactors in addition to DGCR8 (Gregory et al. 2004). Interestingly, two recent studies independently reported alternative splicing of human *DROSHA* exon 7 and found that DROSHA proteins generated from exon 7-skipped isoforms were exclusively nuclear while those from exon 7-containing isoforms were also present in the cytoplasm (Dai et al. 2016; Link et al. 2016). One possibility is that the hydrophobic nature of the exon 7-encoded region may impair nuclear localization or facilitate nuclear export of the protein.

We observed that the ratio of the two splice isoforms resulting from exon 7 alternative splicing varies among different human tissues and that, unlike in other tissues, the exon 7-skipped isoform is dominantly abundant in the brain (Fig. 3B; Supplemental Fig. 3). Indeed, a recent large-scale analysis of RNA-seq data sets from diverse cell and tissue types annotated human *DROSHA* exon 7 as an alternative exon that exhibits increased skipping in neural tissues (Irimia et al. 2014). Mounting evidence suggests that Microprocessor activity and specificity is dynamically regulated in a tissue-specific or developmental stage-specific manner. For example, Microprocessor-mediated processing of pri-miR-7-1 is inhibited in non-neural cells by Musashi homolog 2 (MSI2) and Hu antigen R (HuR), which together bind to and stabilize the hairpin (Choudhury et al. 2013). Phosphorylated methyl-CpG binding protein 2 (MeCP2) interferes with the assembly of the Microprocessor by sequestering DGCR8 and suppresses the expression of a subset of miRNAs, which is alleviated upon neuronal calcium signaling by rapid dephosphorylation of MeCP2 (Cheng et al. 2014). TAR DNA-binding protein (TDP-43) has been reported to control the stability and substrate specificity of the Microprocessor during neuronal differentiation (Kawahara and Mieda-Sato 2012; Di Carlo et al. 2013). Similarly, the recognition and processing of the *DROSHA* hairpin by the Microprocessor may be differentially regulated in a spatiotemporal manner, possibly contributing to the varying degree of exon 7 splicing in different tissues. Further investigation is required to uncover the full extent and the biological significance of this additional layer in the control of human *DROSHA* expression.

MATERIALS AND METHODS

Plasmids

To generate a human *DROSHA* exons 6–8 minigene, the genomic fragment encompassing the first nucleotide of exon 6 to the last nucleotide of exon 8 was amplified from human B lymphoblast genomic DNA (ATCC) and cloned into pGEM-T Easy (Promega). We reduced the size of intron 6 (5558 nt) to 973 nt such that the reduced intron 6 contained nt 1–345 and 4931–5558 of the original sequence. The resulting fragment was subcloned into the HindIII/NotI site of pcDNA3.1 (Thermo Fisher Scientific). A mouse minigene was constructed similarly, with intron 6 (4681 nt) reduced to 969 nt at the orthologous position. A pri-miR-143 expression plasmid was generated by subcloning a genomic fragment corresponding to the miR-143 hairpin with flanking sequences into the HindIII/EcoRI site of pcDNA3.1. pCK-DROSHA-Flag and pCK-Flag-DGCR8 were kindly provided by Dr. V. Narry Kim (Seoul National University). Site-directed mutagenesis was carried out by standard inverse PCR procedures. Primer sequences are listed in Supplemental Table 1.

Cell culture and transfection

HEK293T and HeLa cells were maintained in DMEM (WelGene) supplemented with 10% FBS (WelGene). *DROSHA* KO HCT116 cells (a generous gift from Dr. V. Narry Kim) were cultured in McCoy's 5A media (WelGene) containing 10% FBS. NIH-3T3 cells were grown in DMEM supplemented with 10% BCS (WelGene). All cell lines used in this study were regularly tested for mycoplasma contamination. For RNAi experiments, cells were transfected with 8 nM siRNA using Lipofectamine 2000 (Thermo Fisher Scientific) and incubated for 72 h. The sequences of siRNAs are provided in Supplemental Table 1. Plasmid transfection was performed using Lipofectamine 2000, with 1 μg of minigene plasmid and 2 μg of effector plasmid delivered per 35-mm dish. Cells were harvested 48 h after plasmid transfection.

RNA measurement

Total RNA was prepared using TRI Reagent (Thermo Fisher Scientific), according to the manufacturer's instructions. RNAs

to be reverse transcribed were further treated with Recombinant DNase I (Takara) to remove contaminating genomic DNA. Human tissue RNAs were from the Human Total RNA Master Panel II (Clontech) and were directly used in reverse transcription. 5′ RLM-RACE was performed using the GeneRacer Kit (Thermo Fisher Scientific) with minor modifications. Briefly, 5 µg of DNase-treated total RNA was ligated to 250 ng of GeneRacer RNA Oligo using T4 RNA Ligase (Thermo Fisher Scientific). After phenol extraction and ethanol precipitation, the 5′-ligated RNA was reverse transcribed with random hexamer and PrimeScript Reverse Transcriptase (Takara). PCR amplification was terminated during the linear phase and the PCR products were resolved on a 2% agarose gel. For analysis of splice isoforms, we performed radioactive RT-PCR by including 5′ end-labeled forward primers in reactions at ~20 nM. Densitometric analysis of splice isoforms was carried out using Multi Gauge V3.0 (Fujifilm) or ImageJ (National Institutes of Health) softwares. Quantitative RT-PCR measurement of splice isoforms based on the comparative Ct method with SYBR Green was conducted with LightCycler 480 Instrument II (Roche Life Science). Human *GAPDH* mRNA was amplified as an endogenous control. Primer sequences are listed in Supplemental Table 1. For small RNA Northern blot analysis, 20 µg of total RNA was separated on a 12.5% urea–polyacrylamide gel and transferred to Hybond N+ nylon membrane (GE Healthcare Life Sciences). An antisense oligonucleotide probe corresponding to the *DROSHA* small RNA 5p (5′-UCUUGGGCCCCACCCCUGGAGA-3′) was prepared using the StarFire miRNA Detection Kit (Integrated DNA Technologies). Probes for miR-143, $tRNA^{Lys}$, and U1 snRNA were generated by standard 5′ end-labeling reactions using T4 Polynucleotide Kinase (Takara).

Western blot analysis

Cells were harvested and lysed in RIPA buffer (50 mM Tris-HCl at pH 8.0, 150 mM NaCl, 1% NP-40, 0.5% sodium deoxycholate, 0.1% SDS, 1× cOmplete Protease Inhibitor Cocktail [Roche Life Science]) on ice for 30 min. Thirty to fifty micrograms of lysate were separated on a 10% SDS-polyacrylamide gel and transferred to Immobilon-P PVDF membrane (EMD Millipore). The primary antibodies used in this study were rabbit anti-Flag (Sigma, F7425), rabbit anti-α-tubulin (Abcam, ab52866), mouse anti-hnRNP A1 (4B10; EMD Millipore, 05-1521), rabbit anti-DROSHA (Abcam, ab12286), rabbit anti-DGCR8 (a gift from Dr. V. Narry Kim), and rabbit anti-DICER1 (Abcam, ab13502).

In vitro DROSHA processing and directional cloning of the processing product

Microprocessor lysate was prepared as described elsewhere (Lee and Kim 2007; Auyeung et al. 2013) with minor modifications. Briefly, HEK293T cells cotransfected with pCK-DROSHA-Flag and pCK-Flag-DGCR8 were dispersed in Buffer D (20 mM HEPES-KOH at pH 7.9, 100 mM KCl, 0.2 mM EDTA, 5 mM DTT, 10% glycerol, 1× cOmplete Protease Inhibitor Cocktail) and lysed by sonication. After centrifugation at 15,000 rpm at 4°C for 15 min, the supernatant was collected as Microprocessor lysate. In vitro DROSHA processing was performed in 10-µL reactions containing ~10 nM [α-^{32}P]UTP-labeled RNA substrate, 50% (v/v) of Microprocessor lysate (5 µg/µL), and 6.4 mM $Mg(OAc)_2$ with incubation at 37°C for 30 min. Reactions were quenched by treating with Proteinase K (Roche Life Science) at 60°C for 20 min and then purified by phenol extraction and ethanol precipitation. The reaction products were separated on a 12.5% urea–polyacrylamide gel and analyzed by phosphorimaging (Fujifilm BAS-2500). For directional cloning of the ~60-nt processing product, the corresponding band was gel-purified, sequentially ligated to 3′ and 5′ adaptors, amplified by RT-PCR, and subcloned into pGEM-T Easy.

RNA pulldown assay

RNA pulldown was performed as described elsewhere (Michlewski and Caceres 2010) with minor modifications. One hundred pmoles (~6 µg) of cold hairpin RNA were 3′ oxidized with sodium *m*-periodate (Sigma) and covalently attached to 25 µL of adipic acid dihydrazide agarose beads (Sigma). The beads were extensively washed with 2 M KCl, equilibrated with Buffer D, and then incubated with ~1 mg of Microprocessor lysate in 100-µL reactions in the presence of 1.6 mM $Mg(OAc)_2$ at RT for 2 h with constant rotation. After washing with Buffer D containing 1.6 mM $Mg(OAc)_2$ four times, proteins specifically bound to the RNA were eluted by treating the beads with RNase Cocktail (Thermo Fisher Scientific) at 37°C for 30 min and analyzed by Western blotting.

Psoralen crosslinking assay

HeLa nuclear extract was prepared as previously described (Dignam et al. 1983). For psoralen crosslinking, ~10 nM [α-^{32}P]UTP-labeled RNA substrate was incubated in 10-µL reactions with 50% (v/v) of HeLa nuclear extract, 0.5 mM ATP, 20 mM creatine phosphate, and 1.6 mM $Mg(OAc)_2$ at 30°C for 15 min, supplemented with 2.5 µL of 4′-aminomethyltrioxsalen hydrochloride (200 ng/µL; Sigma) and immediately irradiated with 365-nm UV light for 15 min. Reactions were quenched by treating with Proteinase K (Roche Life Science) at 60°C for 20 min and then purified by phenol extraction and ethanol precipitation. To identify the U1 snRNA:substrate crosslinked species, purified crosslinking products were annealed to a DNA oligonucleotide complementary to U1 snRNA nt 64–75 and treated with RNase H (Thermo Fisher Scientific) at 37°C for 30 min. The crosslinking products were separated on a 6% urea–polyacrylamide gel and analyzed by phosphorimaging (Fujifilm BAS-2500). For the competition assay presented in Figure 5D, 30% (v/v) of mock or Microprocessor lysate (25 µg/µL) prepared from transfected HEK293T cells was supplemented in the crosslinking reactions. The relative intensity of the U1 snRNA:*DROSHA* hairpin adduct was calculated by normalizing the intensity of the adduct by the intensity over the whole lane.

RNA immunoprecipitation

RNA immunoprecipitation was performed as described elsewhere (Niranjanakumari et al. 2002) with minor modifications. Forty-eight hours after transfection, cells were fixed in 0.5% formaldehyde in 1× PBS at RT for 5 min and lysed in RIPA buffer on ice for 30 min. The lysate was further sonicated for 1 min to shear genomic DNA and then centrifuged at 15,000 rpm at 4°C for 15 min. Immunoprecipitation was performed using anti-Flag M2 Affinity Gel (Sigma) at 4°C for 2 h with constant rotation. The beads were washed with high-stringent RIPA buffer (RIPA buffer containing

1 M NaCl and 1 M urea) four times, then with RIPA buffer twice, deproteinized by treating with Proteinase K at 60°C for 20 min, and reverse crosslinked at 70°C for 45 min. Coprecipitated RNA was extracted using TRI Reagent, treated with Recombinant DNase I, and reverse transcribed.

Subcellular fractionation

HEK293T cells from a 60-mm dish were collected and dispersed in 600 µL of 1× PBS containing 0.1% NP-40 by gentle pipetting. Two hundred microliters of the resulting suspension was removed for the whole-cell fraction. The remaining suspension was centrifuged at 2200 rpm at 4°C for 5 min, and 200 µL of the supernatant was taken as the cytoplasmic fraction. The nuclei were washed once with 1 ml of 0.1% NP-40/1× PBS and resuspended in 200 µL of 0.1% NP-40/1× PBS. Each fraction was treated with 1 mL of TRI Reagent and subjected to RNA extraction.

SUPPLEMENTAL MATERIAL

Supplemental material is available for this article.

ACKNOWLEDGMENTS

We are grateful to Dr. V. Narry Kim (Seoul National University) for reagents and helpful discussion. We also thank the members of our laboratory for their critical comments on this manuscript. This work is supported by a grant from the Next-Generation BioGreen 21 Program (no. PJ01101803), Rural Development Administration, Republic of Korea.

Received October 27, 2016; accepted April 6, 2017.

REFERENCES

Agranat-Tamir L, Shomron N, Sperling J, Sperling R. 2014. Interplay between pre-mRNA splicing and microRNA biogenesis within the supraspliceosome. *Nucleic Acids Res* **42:** 4640–4651.

Auyeung VC, Ulitsky I, McGeary SE, Bartel DP. 2013. Beyond secondary structure: primary-sequence determinants license pri-miRNA hairpins for processing. *Cell* **152:** 844–858.

Ballarino M, Pagano F, Girardi E, Morlando M, Cacchiarelli D, Marchioni M, Proudfoot NJ, Bozzoni I. 2009. Coupled RNA processing and transcription of intergenic primary microRNAs. *Mol Cell Biol* **29:** 5632–5638.

Bartel DP. 2009. MicroRNAs: target recognition and regulatory functions. *Cell* **136:** 215–233.

Burger K, Gullerova M. 2015. Swiss army knives: non-canonical functions of nuclear Drosha and Dicer. *Nat Rev Mol Cell Biol* **16:** 417–430.

Cheng TL, Wang Z, Liao Q, Zhu Y, Zhou WH, Xu W, Qiu Z. 2014. MeCP2 suppresses nuclear microRNA processing and dendritic growth by regulating the DGCR8/Drosha complex. *Dev Cell* **28:** 547–560.

Chong MM, Zhang G, Cheloufi S, Neubert TA, Hannon GJ, Littman DR. 2010. Canonical and alternate functions of the microRNA biogenesis machinery. *Genes Dev* **24:** 1951–1960.

Choudhury NR, de Lima Alves F, de Andrés-Aguayo L, Graf T, Cáceres JF, Rappsilber J, Michlewski G. 2013. Tissue-specific control of brain-enriched miR-7 biogenesis. *Genes Dev* **27:** 24–38.

Cirera-Salinas D, Yu J, Bodak M, Ngondo RP, Herbert KM, Ciaudo C. 2017. Noncanonical function of DGCR8 controls mESC exit from pluripotency. *J Cell Biol* **216:** 355–366.

Dai L, Chen K, Youngren B, Kulina J, Yang A, Guo Z, Li J, Yu P, Gu S. 2016. Cytoplasmic Drosha activity generated by alternative splicing. *Nucleic Acids Res* **44:** 10454–10466.

Denli AM, Tops BB, Plasterk RH, Ketting RF, Hannon GJ. 2004. Processing of primary microRNAs by the Microprocessor complex. *Nature* **432:** 231–235.

Di Carlo V, Grossi E, Laneve P, Morlando M, Dini Modigliani S, Ballarino M, Bozzoni I, Caffarelli E. 2013. TDP-43 regulates the microprocessor complex activity during in vitro neuronal differentiation. *Mol Neurobiol* **48:** 952–963.

Dignam JD, Lebovitz RM, Roeder RG. 1983. Accurate transcription initiation by RNA polymerase II in a soluble extract from isolated mammalian nuclei. *Nucleic Acids Res* **11:** 1475–1489.

Fang W, Bartel DP. 2015. The menu of features that define primary microRNAs and enable de novo design of microRNA genes. *Mol Cell* **60:** 131–145.

Gregory RI, Yan KP, Amuthan G, Chendrimada T, Doratotaj B, Cooch N, Shiekhattar R. 2004. The Microprocessor complex mediates the genesis of microRNAs. *Nature* **432:** 235–240.

Grishok A, Pasquinelli AE, Conte D, Li N, Parrish S, Ha I, Baillie DL, Fire A, Ruvkun G, Mello CC. 2001. Genes and mechanisms related to RNA interference regulate expression of the small temporal RNAs that control *C. elegans* developmental timing. *Cell* **106:** 23–34.

Gromak N, Dienstbier M, Macias S, Plass M, Eyras E, Caceres JF, Proudfoot NJ. 2013. Drosha regulates gene expression independently of RNA cleavage function. *Cell Rep* **5:** 1499–1510.

Ha M, Kim VN. 2014. Regulation of microRNA biogenesis. *Nat Rev Mol Cell Biol* **15:** 509–524.

Hammond SM, Boettcher S, Caudy AA, Kobayashi R, Hannon GJ. 2001. Argonaute2, a link between genetic and biochemical analyses of RNAi. *Science* **293:** 1146–1150.

Han J, Lee Y, Yeom KH, Kim YK, Jin H, Kim VN. 2004. The Drosha-DGCR8 complex in primary microRNA processing. *Genes Dev* **18:** 3016–3027.

Han J, Lee Y, Yeom KH, Nam JW, Heo I, Rhee JK, Sohn SY, Cho Y, Zhang BT, Kim VN. 2006. Molecular basis for the recognition of primary microRNAs by the Drosha-DGCR8 complex. *Cell* **125:** 887–901.

Han J, Pedersen JS, Kwon SC, Belair CD, Kim YK, Yeom KH, Yang WY, Haussler D, Blelloch R, Kim VN. 2009. Posttranscriptional crossregulation between Drosha and DGCR8. *Cell* **136:** 75–84.

Havens MA, Reich AA, Hastings ML. 2014. Drosha promotes splicing of a pre-microRNA-like alternative exon. *PLoS Genet* **10:** e1004312.

Heras SR, Macias S, Plass M, Fernandez N, Cano D, Eyras E, Garcia-Perez JL, Caceres JF. 2013. The Microprocessor controls the activity of mammalian retrotransposons. *Nat Struct Mol Biol* **20:** 1173–1181.

Hutvagner G, McLachlan J, Pasquinelli AE, Balint E, Tuschl T, Zamore PD. 2001. A cellular function for the RNA-interference enzyme Dicer in the maturation of the let-7 small temporal RNA. *Science* **293:** 834–838.

Irimia M, Weatheritt RJ, Ellis JD, Parikshak NN, Gonatopoulos-Pournatzis T, Babor M, Quesnel-Vallieres M, Tapial J, Raj B, O'Hanlon D, et al. 2014. A highly conserved program of neuronal microexons is misregulated in autistic brains. *Cell* **159:** 1511–1523.

Janas MM, Khaled M, Schubert S, Bernstein JG, Golan D, Veguilla RA, Fisher DE, Shomron N, Levy C, Novina CD. 2011. Feed-forward microprocessing and splicing activities at a microRNA-containing intron. *PLoS Genet* **7:** e1002330.

Jin Y, Yang Y, Zhang P. 2011. New insights into RNA secondary structure in the alternative splicing of pre-mRNAs. *RNA Biol* **8:** 450–457.

Johanson TM, Keown AA, Cmero M, Yeo JH, Kumar A, Lew AM, Zhan Y, Chong MM. 2015. Drosha controls dendritic cell development by cleaving messenger RNAs encoding inhibitors of myelopoiesis. *Nat Immunol* **16:** 1134–1141.

Kadener S, Rodriguez J, Abruzzi KC, Khodor YL, Sugino K, Marr MT II, Nelson S, Rosbash M. 2009. Genome-wide identification of targets of the drosha-pasha/DGCR8 complex. *RNA* **15:** 537–545.

Karginov FV, Cheloufi S, Chong MM, Stark A, Smith AD, Hannon GJ. 2010. Diverse endonucleolytic cleavage sites in the mammalian

transcriptome depend upon microRNAs, Drosha, and additional nucleases. *Mol Cell* **38:** 781–788.
Kataoka N, Fujita M, Ohno M. 2009. Functional association of the Microprocessor complex with the spliceosome. *Mol Cell Biol* **29:** 3243–3254.
Kawahara Y, Mieda-Sato A. 2012. TDP-43 promotes microRNA biogenesis as a component of the Drosha and Dicer complexes. *Proc Natl Acad Sci* **109:** 3347–3352.
Kim YK, Kim VN. 2007. Processing of intronic microRNAs. *EMBO J* **26:** 775–783.
Kim YK, Kim B, Kim VN. 2016. Re-evaluation of the roles of DROSHA, Export in 5, and DICER in microRNA biogenesis. *Proc Natl Acad Sci* **113:** E1881–1889.
Knuckles P, Vogt MA, Lugert S, Milo M, Chong MM, Hautbergue GM, Wilson SA, Littman DR, Taylor V. 2012. Drosha regulates neurogenesis by controlling neurogenin 2 expression independent of microRNAs. *Nat Neurosci* **15:** 962–969.
Kwon SC, Nguyen TA, Choi YG, Jo MH, Hohng S, Kim VN, Woo JS. 2016. Structure of Human DROSHA. *Cell* **164:** 81–90.
Lee Y, Kim VN. 2007. In vitro and in vivo assays for the activity of Drosha complex. *Methods Enzymol* **427:** 89–106.
Lee Y, Ahn C, Han J, Choi H, Kim J, Yim J, Lee J, Provost P, Radmark O, Kim S, et al. 2003. The nuclear RNase III Drosha initiates microRNA processing. *Nature* **425:** 415–419.
Lin YT, Sullivan CS. 2011. Expanding the role of Drosha to the regulation of viral gene expression. *Proc Natl Acad Sci* **108:** 11229–11234.
Link S, Grund SE, Diederichs S. 2016. Alternative splicing affects the subcellular localization of Drosha. *Nucleic Acids Res* **44:** 5330–5343.
Long JC, Caceres JF. 2009. The SR protein family of splicing factors: master regulators of gene expression. *Biochem J* **417:** 15–27.
Lujambio A, Lowe SW. 2012. The microcosmos of cancer. *Nature* **482:** 347–355.
Macias S, Plass M, Stajuda A, Michlewski G, Eyras E, Caceres JF. 2012. DGCR8 HITS-CLIP reveals novel functions for the Microprocessor. *Nat Struct Mol Biol* **19:** 760–766.
Marinaro F, Marzi MJ, Hoffmann N, Amin H, Pelizzoli R, Niola F, Nicassio F, De Pietri Tonelli D. 2017. MicroRNA-independent functions of DGCR8 are essential for neocortical development and TBR1 expression. *EMBO Rep* **18:** 603–618.
Mattioli C, Pianigiani G, Pagani F. 2013. A competitive regulatory mechanism discriminates between juxtaposed splice sites and pri-miRNA structures. *Nucleic Acids Res* **41:** 8680–8691.
McManus CJ, Graveley BR. 2011. RNA structure and the mechanisms of alternative splicing. *Curr Opin Genet Dev* **21:** 373–379.
Melamed Z, Levy A, Ashwal-Fluss R, Lev-Maor G, Mekahel K, Atias N, Gilad S, Sharan R, Levy C, Kadener S, et al. 2013. Alternative splicing regulates biogenesis of miRNAs located across exon-intron junctions. *Mol Cell* **50:** 869–881.
Michlewski G, Caceres JF. 2010. RNase-assisted RNA chromatography. *RNA* **16:** 1673–1678.
Morlando M, Ballarino M, Gromak N, Pagano F, Bozzoni I, Proudfoot NJ. 2008. Primary microRNA transcripts are processed co-transcriptionally. *Nat Struct Mol Biol* **15:** 902–909.
Mourelatos Z, Dostie J, Paushkin S, Sharma A, Charroux B, Abel L, Rappsilber J, Mann M, Dreyfuss G. 2002. miRNPs: a novel class of ribonucleoproteins containing numerous microRNAs. *Genes Dev* **16:** 720–728.
Nguyen TA, Jo MH, Choi YG, Park J, Kwon SC, Hohng S, Kim VN, Woo JS. 2015. Functional anatomy of the human microprocessor. *Cell* **161:** 1374–1387.
Nilsen TW. 2014. Detecting RNA-RNA interactions using psoralen derivatives. *Cold Spring Harb Protoc* **2014:** 996–1000.
Niranjanakumari S, Lasda E, Brazas R, Garcia-Blanco MA. 2002. Reversible cross-linking combined with immunoprecipitation to study RNA-protein interactions in vivo. *Methods* **26:** 182–190.
Pawlicki JM, Steitz JA. 2010. Nuclear networking fashions pre-messenger RNA and primary microRNA transcripts for function. *Trends Cell Biol* **20:** 52–61.
Piriyapongsa J, Marino-Ramirez L, Jordan IK. 2007. Origin and evolution of human microRNAs from transposable elements. *Genetics* **176:** 1323–1337.
Qin S, Jin P, Zhou X, Chen L, Ma F. 2015. The role of transposable elements in the origin and evolution of microRNAs in human. *PLoS One* **10:** e0131365.
Roberts JT, Cardin SE, Borchert GM. 2014. Burgeoning evidence indicates that microRNAs were initially formed from transposable element sequences. *Mob Genet Elements* **4:** e29255.
Shepard PJ, Hertel KJ. 2009. The SR protein family. *Genome Biol* **10:** 242.
Shin C, Nam JW, Farh KK, Chiang HR, Shkumatava A, Bartel DP. 2010. Expanding the microRNA targeting code: functional sites with centered pairing. *Mol Cell* **38:** 789–802.
Tang X, Zhang Y, Tucker L, Ramratnam B. 2010. Phosphorylation of the RNase III enzyme Drosha at Serine300 or Serine302 is required for its nuclear localization. *Nucleic Acids Res* **38:** 6610–6619.
Tang X, Li M, Tucker L, Ramratnam B. 2011. Glycogen synthase kinase 3 β (GSK3β) phosphorylates the RNAase III enzyme Drosha at S300 and S302. *PLoS One* **6:** e20391.
Tang X, Wen S, Zheng D, Tucker L, Cao L, Pantazatos D, Moss SF, Ramratnam B. 2013. Acetylation of Drosha on the N-terminus inhibits its degradation by ubiquitination. *PLoS One* **8:** e72503.
Triboulet R, Chang HM, Lapierre RJ, Gregory RI. 2009. Post-transcriptional control of DGCR8 expression by the Microprocessor. *RNA* **15:** 1005–1011.
Yang Q, Li W, She H, Dou J, Duong DM, Du Y, Yang SH, Seyfried NT, Fu H, Gao G, et al. 2015. Stress induces p38 MAPK-mediated phosphorylation and inhibition of Drosha-dependent cell survival. *Mol Cell* **57:** 721–734.
Yuan Z, Sun X, Jiang D, Ding Y, Lu Z, Gong L, Liu H, Xie J. 2010. Origin and evolution of a placental-specific microRNA family in the human genome. *BMC Evol Biol* **10:** 346.
Zeng Y, Yi R, Cullen BR. 2005. Recognition and cleavage of primary microRNA precursors by the nuclear processing enzyme Drosha. *EMBO J* **24:** 138–148.
Zuker M. 2003. Mfold web server for nucleic acid folding and hybridization prediction. *Nucleic Acids Res* **31:** 3406–3415.